CRYSTAL GROWTH & DESIGN

Article

Cite This: Cryst. Growth Des. 2019, 19, 6743−6751

pubs.acs.org/crystal

Metal Ion Effects on Fullerene/Porphyrin Cocrystallization

Mrittika Roy, Marilyn M. Olmstead,* and Alan L. Balch*

Department of Chemistry, University of California, Davis, California 95616, United States

Supporting Information

ABSTRACT: This investigation presents a systematic examination of the late transition metal octaethylporphyrins M^{II}(OEP) with M = Co, Ni, Cu, and Zn as cocrystallization agents for C_{60}. In each case, the fullerene was dissolved in benzene and then layered over an equimolar dichloromethane solution of the porphyrin. A striking new columnar structural type for these systems is found for Co^{II}(OEP) and Zn^{II}(OEP) with stoichiometric ratios 6:5 for porphyrin/fullerene. In these cocrystals, one fullerene is surrounded by two porphyrins, one is adjacent to only one porphyrin, while one makes no contact with a porphyrin; yet, all three fullerenes are ordered at 90 K. A more typical, also new, 1:1 structure with Cu^{II}(OEP) and C_{60} shows back-to-back porphyrins with all eight ethyl groups embracing the fullerene. In these three structures only dichloromethane is found as the solvate. The Ni^{II}(OEP) structure is related to the known structure of Ni^{II}(OEP)·C_{60}·$2C_6H_6$ but has incorporated ca. 5% dichloromethane. In these Ni^{II}(OEP)/C_{60} cocrystals, four of the ethyl groups embrace the fullerene, while the other four are displaced to the opposite side of the porphyrin plane where they do not make contact with a fullerene. The porphyrin core conformations of the different metal derivatives also differ, and their possible impact on cocrystal formation is discussed.

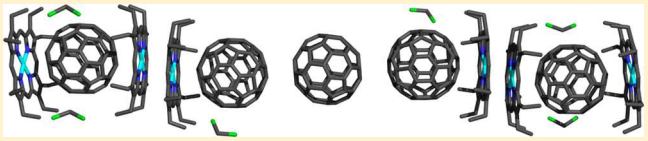

INTRODUCTION

Since the discovery of fullerenes[1] and endohedral fullerenes[2] and their isolation as solid materials,[3] the structures of these unusual molecules have attracted attention.[4] Single-crystal X-ray diffraction provides definitive, three-dimensional structural information about these molecules. However, the rather undifferentiated exteriors of these molecules with a pattern of only pentagons and hexagons produce situations in which crystal disorder is common. The initial solution to the disorder issue involved external functionalization with transition metal complexes. Such functionalization lowered the symmetry of the molecules and produced ordered crystals that led to the structural characterization of C_{60},[5,6] C_{70},[7] and C_{84}[8] in three dimensions. However, the formation of adducts can result in significant modification of the cage structure. Consequently, a crystallization method that leaves the cage structure unaltered is more desirable.

Cocrystallization of fullerenes with bowl-like molecules represents one means of obtaining crystals that are free of orientational disorder. Thus, the bowl-shaped hydrocarbon dibenzo[a,g]corannulene forms ordered crystals with C_{60} and with C_{70}.[9] Similarly, another bowl-like molecule, hexakis[(*E*)-3,3-dimethyl-1-butenyl]benzene, also forms ordered cocrystals with C_{60}.[10] Another curved molecule, the conical tetrabenzoquadrannulene cocrystallizes with C_{60} to produce a solid containing two different fullerene molecules nested within tetrabenzoquadrannulene molecules.[11] Here, one of the C_{60} molecules is ordered, while the other displays a degree of disorder. Unfortunately, these bowl-like molecules are not readily available, and more readily accessible cocrystallization agents have come to be useful. Remarkably, the flat surfaces of porphyrins have an affinity to crystallize with fullerenes.

Cocrystallization of fullerenes and metallofullerenes with M^{II}(OEP), particularly Ni(OEP), has been used to obtain suitable ordered crystals for single-crystal X-ray diffraction study of these difficult to crystallize molecules.[12,13] This methodology has facilitated the discovery of novel carbon cages (e.g., endohedral fullerenes that contain heptagons[14,15] or three adjacent pentagons[16]) and the structure of unusual clusters inside these cages (e.g., $Sc_4O_2@I_h$-C_{80},[17] $Sc_4O_3@I_h$-C_{80},[18] and $Sc_2(\mu_2\text{-}O)@C_s(6)$-$C_{82}$[19]). Cocrystallization with M^{II}(OEP) has been utilized worldwide for the structure determination of a wide variety of fullerenes and endohedral fullerenes.[20−28]

Although the use of cocrystallization of M^{II}(OEP) with fullerenes is widely used, there are several issues regarding the supramolecular interactions within these crystals that remain poorly understood. For example, there are cases where a C_{60} molecule can be surrounded by one, two, or three porphyrin molecules.[9,29,30] Usually, a M^{II}(OEP) molecule interacts with a fullerene on only one side, but there are cases where a M^{II}(OEP) molecule is sandwiched between two fullerenes.[31] Here, we report some systematic studies of the cocrystallization of C_{60} with M^{II}(OEP) with M = Co, Ni, Cu, and Zn that probe the effects of altering the metal ion within the porphyrin on the nature of the cocrystals that form.

RESULTS AND DISCUSSION

Cocrystal Growth. Crystals of $6Co^{II}$(OEP)·$5C_{60}$·$5CH_2Cl_2$ (**1**), $6Zn^{II}$(OEP)·$5C_{60}$·$5CH_2Cl_2$ (**2**), Cu^{II}(OEP)·C_{60}·CH_2Cl_2

Received: August 14, 2019
Revised: September 10, 2019
Published: September 18, 2019

DOI: 10.1021/acs.cgd.9b01092
Cryst. Growth Des. 2019, 19, 6743−6751

(3), and $Ni^{II}(OEP)\cdot C_{60}\cdot 0.1CH_2Cl_2\cdot 1.9C_6H_6$ (4) were prepared by a common procedure that involved layering a solution of C_{60} in benzene over an equimolar solution of the appropriate $M^{II}(OEP)$ in dichloromethane or the reverse. Crystals started appearing within 24 h, but they were allowed to grow for about 2 weeks to achieve the size we wanted for data collection. As done in previous studies,[32,33] we carefully examined the morphology and diffraction from many crystals for each of the four different cocrystals. Only one type of cocrystal was found for each of the four different metalloporphyrins. Crystallographic data for the four crystals are shown in Table 1. Efforts to obtain crystals with different compositions by increasing the $M^{II}(OEP)/C_{60}$ ratio produced only the four cocrystals reported here. With large excesses of $M^{II}(OEP)$, crystals of pristine porphyrin formed alongside cocrystals listed in Table 1. A similar process using a dichloroethane solution of the appropriate $Co^{II}(OEP)$ or $Zn^{II}(OEP)$ was used to produce the cocrystals $6Co^{II}(OEP)\cdot 5C_{60}\cdot 5C_2H_4Cl_2$ and $6Zn^{II}(OEP)\cdot 5C_{60}\cdot 5C_2H_4Cl_2$.

Structure of $6Co^{II}(OEP)\cdot 5C_{60}\cdot 5CH_2Cl_2$ (1). The crystals form in the space group $P\bar{1}$. The asymmetric unit contains three molecules of $Co^{II}(OEP)$ in general positions, two molecules of C_{60} in general positions, with another half molecule of C_{60} residing on a crystallographic inversion center, and disordered molecules of dichloromethane at three sites. (Because of partial occupancies, the formula only designates five molecules of dichloromethane, although six sites are in use.) Part A of Figure 1 shows a drawing of the asymmetric unit with each fullerene shown in a distinctive color. There are three different environments for the fullerenes in this crystal. As seen in part A of Figure 1, the red-colored fullerene is seated between two porphyrins (reminiscent of a clamshell arrangement observed previously). The blue-colored fullerene is capped at one end by a porphyrin (suggestive of the commonly seen 1:1 fullerene/porphyrin stoichiometry) and abuts another fullerene on the opposite side. Remarkably, the yellow-colored fullerene, which is located on a center of symmetry, has no neighboring porphyrin. Surprisingly, all three fullerenes are completely ordered at 90 K. These fullerene and porphyrin molecules are arranged into chains as shown in part B of Figure 1. Within this chain, there are two crystallographic centers of symmetry, one situated between two $Co^{II}(OEP)$ molecules and the other at the center of the yellow-colored C_{60} molecule. The solvate molecules, which are not shown in the figure, reside alongside these chains in the spaces between them. The central (yellow) fullerene resides in the center of an octahedron of six adjacent fullerene neighbors. At the axial positions are two blue neighbors with centroid···centroid separation of 9.757 Å, and in the equatorial positions there are two trans red neighbors at centroid···centroid distances of 10.073 and two more trans red cages at 10.139 Å. The packing may be envisioned as a 3-D arrangement of the rows that are shown in Figure 1B, shifted such that a yellow cage always faces the "open" side of a red cage.

It is quite unusual to find a fullerene, like the yellow-colored fullerene, which is situated on a crystallographic symmetry element that coincides with a symmetry element within the fullerene itself. It is much more common to find a fullerene that is position on a crystallographic mirror plane that does not coincide with a mirror plane of the carbon cage. In such a case, the fullerene suffers from disorder with two molecules occupying a common site.[34,35]

Table 1. Crystal Data for Cocrystals[a]

	$6Co^{II}(OEP)\cdot 5C_{60}\cdot 5CH_2Cl_2$ (1)	$6Zn^{II}(OEP)\cdot 5C_{60}\cdot 5CH_2Cl_2$ (2)
chemical formula	$C_{521}H_{270}N_{24}Cl_{10}Co_6$	$C_{521}H_{274}N_{24}Cl_{10}Zn_6$
formula weight	7573.67	7616.34
radiation source, λ (Å)	Mo (Kα), 0.7107	synchrotron, 0.7288
crystal system	triclinic	triclinic
space group	$P\bar{1}$	$P\bar{1}$
T (K)	90 (2)	90 (2)
a (Å)	14.813 (2)	14.7535 (7)
b (Å)	22.313 (3)	22.1632 (11)
c (Å)	27.425 (6)	27.9212 (13)
α (deg)	111.216 (4)	110.6224 (18)
β (deg)	104.646 (5)	105.3385 (18)
γ (deg)	90.245 (3)	90.1696 (19)
V (Å^3)	8129.4(2)	8193.5 (7)
Z	1	1
d_{calc} (Mg m^{-3})	1.547	1.544
μ (mm^{-1})	0.461	0.631
$F(000)$	3896	3918
crystal size, mm	0.406 × 0.178 × 0.086	0.076 × 0.024 × 0.020
reflections collected	311938	196028
data/restraints/parameters	30855/554/2545	43152/1179/2315
R(int)	0.0744	0.0803
R_1 [data with $I > 2\sigma(I)$]	0.1323	0.1122
wR_2 (all data)	0.3258	0.315
largest diff peak, hole (e·Å^{-3})	2.049 and −1.783	3.502 and −2.318
	$Cu^{II}(OEP)\cdot C_{60}\cdot CH_2Cl_2$ (3)	$Ni^{II}(OEP)\cdot C_{60}\cdot 1.9C_6H_6\cdot 0.1CH_2Cl_2$ (4)
chemical formula	$C_{97}H_{46}N_4Cl_2Cu$	$C_{107.4}H_{55.5}N_4Cl_{0.2}Ni$
formula weight	1401.82	1469.16
radiation source, λ (Å)	Mo (Kα), 0.7107	Mo (Kα), 0.7107
crystal system	monoclinic	triclinic
space group	$P2_1/c$	$P\bar{1}$
T (K)	90 (2)	90 (2)
a (Å)	17.158 (2)	14.1211 (5)
b (Å)	14.826 (2)	14.3756 (4)
c (Å)	24.665 (3)	17.1970 (5)
α (deg)	90	87.4514 (11)
β (deg)	107.553 (2)	75.7612 (12)
γ (deg)	90	75.6007 (12)
V (Å^3)	5982.6 (14)	3276.92(18)
Z	4	2
d_{calc} (Mg m^{-3})	1.556	1.489
μ (mm^{-1})	0.519	0.371
$F(000)$	2876	1520
crystal size, mm	0.030 × 0.040 × 0.100	0.840 × 0.710 × 0.470
reflections collected	70627	55000
data/restraints/parameters	21593/4/942	15109/0/1039
R(int)	0.0748	0.0213
R_1 [data with $I > 2\sigma(I)$]	0.0664	0.0330
wR_2 (all data)	0.1868	0.0856
largest diff peak, hole (e·Å^{-3})	2.596 and −1.542	0.700 and −0.556

[a] $R_1 = \frac{\Sigma \| Fo \| - \| Fc \|}{\Sigma |Fo|}$; $wR_2 = \left\{ \frac{\Sigma [w(Fo^2 - Fc^2)^2]}{\Sigma [w(Fo^2)^2]} \right\}^{1/2}$

DOI: 10.1021/acs.cgd.9b01092
Cryst. Growth Des. 2019, 19, 6743−6751

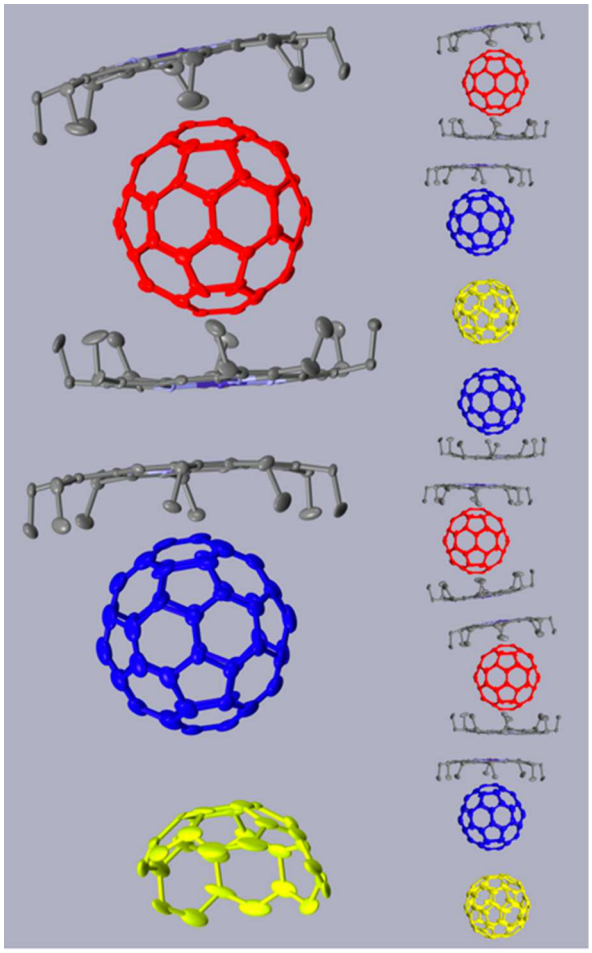

Figure 1. Organization of fullerenes and $Co^{II}(OEP)$·molecules in $6Co^{II}(OEP)·5C_{60}·5CH_2Cl_2$ (**1**). The asymmetric unit is shown in A, while a column of three asymmetric units, with an additional half of a yellow C_{60} molecule at the bottom, is shown in B. Solvate molecules, which reside on the sides of these chains, and hydrogen atoms are omitted for clarity.

The thermal ellipsoids of the three different C_{60} molecules show an interesting trend. The average isotropic thermal ellipsoid for the red fullerene in Figure 1, which is sandwiched between two porphyrins, is 0.0388 $Å^2$, while that for the blue fullerene that is encapsulated by only on porphyrin is larger, 0.0521 $Å^2$. The yellow C_{60} molecule, which does not interact with a porphyrin, has an even larger average thermal ellipsoid, 0.0636 $Å^2$. These differences indicate that the adjacency of the porphyrin acts to restrict the thermal motion of the neighboring fullerene. Computational studies have shown that complementary regions of surface charge on the porphyrin and the fullerene are involved in producing ordered fullerene molecules in these crystals.[36,37]

Along the chains shown in Figure 1, the $Co^{II}(OEP)$ molecules have all eight ethyl groups arranged to embrace the adjacent C_{60} molecule. Additionally, the $Co^{II}(OEP)$ molecules occur as back-to-back pairs. Some of the distances between these paired $Co^{II}(OEP)$ molecules are given in Table 2.

During data collection, it was apparent that the crystal of $6Co^{II}(OEP)·5C_{60}·5CH_2Cl_2$ underwent a phase change upon cooling. At 140 K, the crystal was monoclinic (space group $C2/m$) but displayed disorder that was particularly pronounced for the C_{60} molecule that was not adjacent to a porphyrin. On cooling to 90 K, the crystal transformed into the twinned, triclinic form as reported in Table 1. In this form, all of the fullerenes are ordered.

Table 2. Distances Between Porphyrins

compound	porphyrin–porphyrin contact	metal–metal distance (Å)	interplanar distance (Å)	lateral shift (Å)
$6Co^{II}(OEP)·5C_{60}·5CH_2Cl_2$ (**1**)	2–3 back-to-back	3.435	2.905	1.833
	1–1 across inversion center	3.305	3.163	0.958
$6Zn^{II}(OEP)·5C_{60}·5CH_2Cl_2$ (**2**)	2–3 back-to-back	3.118	3.058	0.611
	1–1 across inversion center	3.084	3.144	1.903
$Cu^{II}(OEP)·C_6·CH_2Cl_2$ (**3**)	1–1 back-to-back	3.399	3.226	1.071
$Ni^{II}(OEP)·C_{60}·0.1CH_2Cl_2·1.9C_6H_6$ (**4**)	1–1 back-to-back	4.690	3.520	3.099

Structure of $6Zn^{II}(OEP)·5C_{60}·5CH_2Cl_2$ (2). Crystals of $6Zn^{II}(OEP)·5C_{60}·5CH_2Cl_2$ (**2**) are nominally isostructural with those of $6Co^{II}(OEP)·5C_{60}·5CH_2Cl_2$ (**1**) as seen from the data in Table 1. The asymmetric unit, which is shown in Figure 2, consists of three molecules of $Zn^{II}(OEP)$ and two molecules of C_{60} in general positions along with a half molecule of C_{60} residing on a crystallographic inversion center. There are also 2.5 molecules of dichloromethane spread over three sites. The thermal ellipsoids of the three different C_{60} molecules again show variations. The yellow C_{60} molecule, which does not interact with a porphyrin, has the largest average isotropic thermal sphere, 0.0637 $Å^2$. In contrast, the red C_{60} molecule has an average isotropic thermal parameter of 0.0461 $Å^2$, and the blue fullerene has an average isotropic thermal parameter of 0.0436 $Å^2$. Additionally, there is disorder in the yellow C_{60} molecule that appears to result from incomplete conversion from the high temperature monoclinic form into the twinned, triclinic form.

However, there are two significant differences between the structures of the zinc and cobalt crystals. In $6Zn^{II}(OEP)·5C_{60}·5CH_2Cl_2$ (**2**), one of the 24 ethyl groups is pointing away from the adjacent fullerene, while the others encapsulate a C_{60} molecule. The unique ethyl group is colored green in Figure 2.

The second difference involves the pairwise interactions of $M^{II}(OEP)$ molecules in the two different crystals. In $6Zn^{II}(OEP)·5C_{60}·5CH_2Cl_2$ (**2**), back-to-back porphyrins approach each other much more closely than is the case in the cobalt crystal. Figure 3 shows both sets of adjacent $Zn^{II}(OEP)$ molecules in the crystal. The first set is generated by a center of inversion. For comparison the Co···N distances are 2.939(6) and 2.936(6) Å in one pair and 2.876(6) Å in the other pair in $6Co^{II}(OEP)·5C_{60}·5CH_2Cl_2$ (**1**). Analogous pairwise intermolecular Zn···N distances occur in the structures of $Zn^{II}(OEP)·C_{60}·2C_6H_4Cl_2$ (2.613 Å)[38] and in $2Zn^{II}(OEP)·C_{60}·CHCl_3$ (2.592 and 2.674 Å).[9] These Zn···N distances may be related to the tendency of Zn porphyrins to expand its coordination number, since 61% of those in the Cambridge Structural Database[39] are five-coordinate, whereas, for comparison, 95% of Ni porphyrins are four-coordinate. However, the Zn···N

DOI: 10.1021/acs.cgd.9b01092
Cryst. Growth Des. 2019, 19, 6743–6751

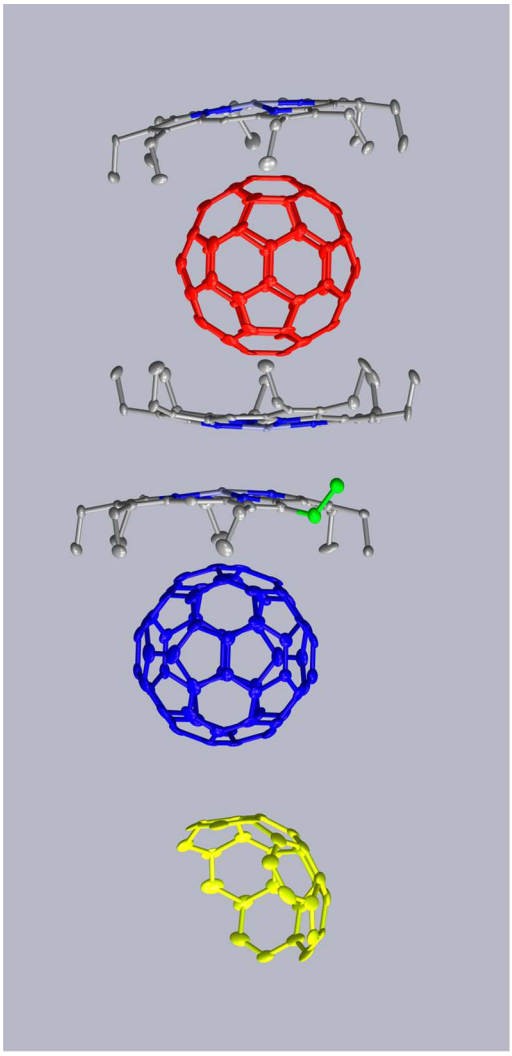

Figure 2. Asymmetric unit in $6Zn^{II}(OEP)\cdot5C_{60}\cdot5CH_2Cl_2$ (**2**). The ethyl group shown in green, which is not directed toward the adjacent fullerene, provides a key difference between this structure and that of $6Co^{II}(OEP)\cdot5C_{60}\cdot5CH_2Cl_2$ (**1**). Solvent molecules, which reside on the sides of these chains, and hydrogen atoms were omitted for clarity.

distances remain significantly longer than the out-of-plane Zn–N(pyridine) distance of 2.200(3) Å in (pyridine)Zn^{II}(OEP).[40]

Structures of the Dichloroethane Solvates: $6Co^{II}(OEP)\cdot5C_{60}\cdot5C_2H_4Cl_2$ (5) and $6Zn^{II}(OEP)\cdot5C_{60}\cdot5C_2H_4Cl_2$ (6). Because of the curious differences between the dichloromethane solvates, $6Co^{II}(OEP)\cdot5C_{60}\cdot5CH_2Cl_2$ (**1**) and $6Zn^{II}(OEP)\cdot5C_{60}\cdot5CH_2Cl_2$ (**2**), where the zinc compound has one ethyl group in one porphyrin directed away from the neighboring fullerene, we examined the growth and structures of similar crystals from dichloroethane/benzene mixtures. The crystals of $6Co^{II}(OEP)\cdot5C_{60}\cdot5C_2H_4Cl_2$ (**5**) and $6Zn^{II}(OEP)\cdot5C_{60}\cdot5C_2H_4Cl_2$ (**6**) that were obtained showed a similar behavior. At 90 K, the crystal system is triclinic, space group $P\bar{1}$, and at 140 K it is monoclinic, space group $C2/m$. In the cobalt compound, all ethyl groups are directed toward the adjoining fullerene. However, in the zinc-containing crystals, one ethyl arm in one of the three Zn^{II}(OEP) molecules is directed away from the fullerene as is the case for $6Zn^{II}(OEP)\cdot5C_{60}\cdot5CH_2Cl_2$ (**2**). Crystallographic data for these two cocrystals are given in the Supporting Information.

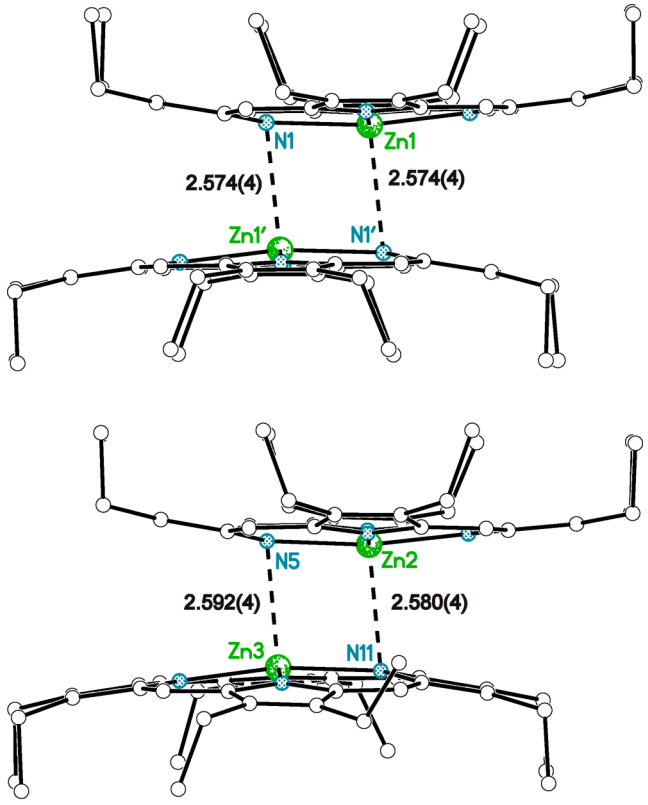

Figure 3. Interaction of two Zn^{II}(OEP) molecules in crystalline $6Zn^{II}(OEP)\cdot5C_{60}\cdot5CH_2Cl_2$ (**2**). Hydrogen atoms are omitted for clarity.

Structure of $Cu^{II}(OEP)\cdot C_{60}\cdot CH_2Cl_2$ (3). The asymmetric unit consists of an ordered C_{60} molecule and a Cu^{II}(OEP) molecule in general positions and a disordered molecule of dichloromethane. Figure 4 shows how the C_{60} and Cu^{II}(OEP) molecules are arranged into chains. The solvate molecules are arranged beside these chains. All eight ethyl groups of the porphyrin embrace the fullerene. There are pairs of Cu^{II}(OEP) molecules in a back-to-back arrangement that are not strongly interacting with one another. The centroid···centroid distance between C_{60} cages in the center of the column depicted in Figure 4 is 9.898 Å. Zigzag chains of C_{60} also pack along the b direction with centroid···centroid separations of 10.132 Å. Dichloromethane molecules occupy interstitial positions.

Structure of $Ni^{II}(OEP)\cdot C_{60}\cdot0.1CH_2Cl_2\cdot1.9C_6H_6$ (4). The asymmetric unit consists of an ordered C_{60} molecule, a Ni^{II}(OEP) molecule, a molecule of benzene, and a second site that is fractionally occupied by 0.1 dichloromethane/0.9benzene. Of the cocrystals reported here, this is the only one to incorporate benzene. Only four of the ethyl groups of a Ni^{II}(OEP) molecule engage the fullerene. The other four reside on the opposite side of the porphyrin plane. Figure 5 shows how the C_{60} and Ni^{II}(OEP) molecules and the solvate molecules are arranged in the solid. Notice that the Ni^{II}(OEP) molecules still adopt a back-to-back arrangement, but as the data in Table 2 show, the Ni···Ni separation and the lateral shift of the porphyrins are much greater than in any of the other cocrystals reported here. In $Ni^{II}(OEP)\cdot C_{60}\cdot0.1CH_2Cl_2\cdot1.9C_6H_6$ the porphyrin has a ruffled distortion that has the largest deviation from planarity of any of the porphyrins reported here as seen in Figure 6. Related cocrystals, $Ni^{II}(OEP)\cdot C_{60}\cdot2C_6H_6$ and $Ni^{II}(OEP)\cdot0.09Kr@C_{60}/0.91C_{60}\cdot$

DOI: 10.1021/acs.cgd.9b01092
Cryst. Growth Des. 2019, 19, 6743–6751

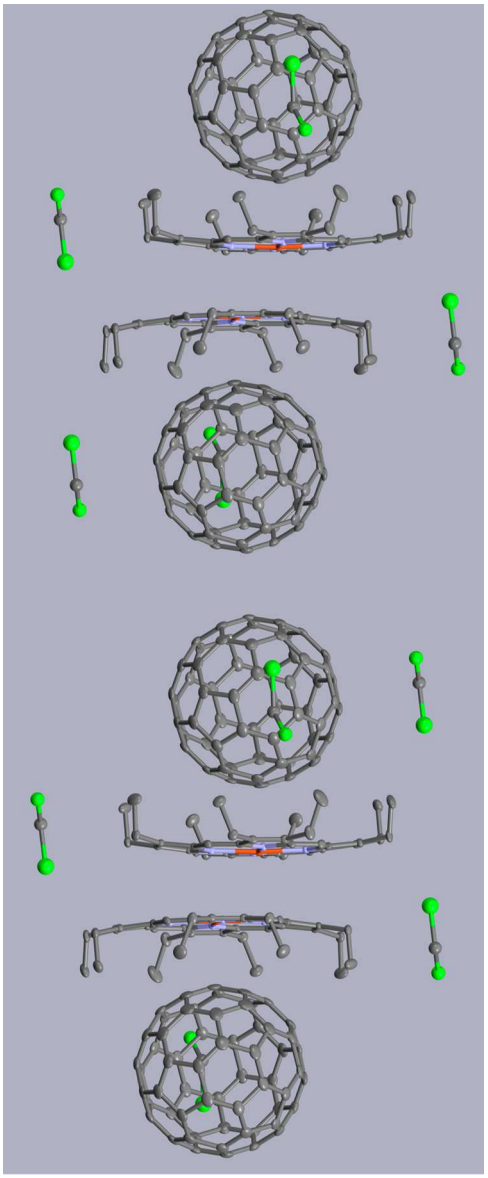

Figure 4. Columnar structure of $Cu^{II}(OEP)\cdot C_{60}\cdot CH_2Cl_2$ (**3**) parallel to *c*. The positions of solvate molecules are included, but hydrogen atoms and the disorder in the dichloromethane molecules are omitted for clarity.

$2C_6H_6$, with similar structures were reported earlier.[41] Recently, the cocrystal $Ni^{II}(OEP)\cdot CH_4@C_{60}\cdot 2C_6H_6$, with methane trapped inside C_{60}, was found to have an analogous structure.[18] Additionally, $Pd^{II}(OEP)\cdot C_{60}\cdot 1.5C_6H_6$ and $Cu^{II}(OEP)\cdot C_{60}\cdot 2C_6H_6$ have similar structures with only four ethyl groups of the porphyrin contacting the fullerene and with an analogous back-to-back arrangement of two porphyrins.[42]

Comparisons of Metalloporphyrin Structures. The porphyrins in each of the cocrystals reported here show some differences that depend upon the metal involved. Table 3 lists the metal−nitrogen distances in the cocrystals. These distances decrease in the following order: Zn-N > Cu-N > Co-N > Ni−N. Deviations of the metal from the least-squares N4 plane are also listed.

In these cocrystals, the porphyrin macrocycles are distorted from planarity. Porphyrin distortions have been classified as ruffed, saddled, domed, waved, or pyrrole propellered.[43] Figure 7 shows diagrams that compare the out-of-plane displacements of the porphyrin core atoms from the mean plane of the porphyrin for $6Co^{II}(OEP)\cdot 5C_{60}\cdot 5CH_2Cl_2$(**1**), $6Zn^{II}(OEP)\cdot 5C_{60}\cdot 5CH_2Cl_2$ (**2**), $Cu^{II}(OEP)\cdot C_{60}\cdot CH_2Cl_2$ (**3**), and $Ni^{II}(OEP)\cdot C_{60}\cdot 0.1CH_2Cl_2\cdot 1.9C_6H_6$ (**4**). Figure 7 presents similar data from the crystal structures of the pristine complexes $M^{II}(OEP)$: triclinic $Co^{II}(OEP)$,[44] triclinic $Zn^{II}(OEP)$,[45] triclinic $Cu^{II}(OEP)$,[46] triclinic A $Ni^{II}(OEP)$,[47] triclinic B $Ni^{II}(OEP)$,[48] tetragonal $Ni^{II}(OEP)$,[49] and monoclinic (*C*2/*c*) $Ni^{II}(OEP)$.[50]

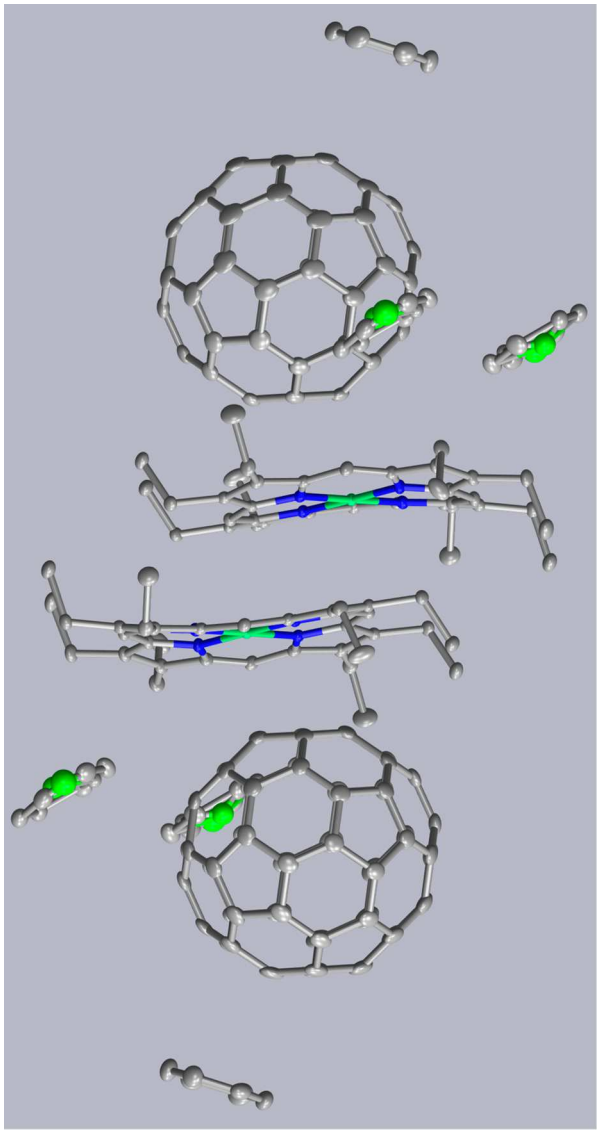

Figure 5. Orientations of the porphyrins, fullerenes and solvate molecules in $Ni^{II}(OEP)\cdot C_{60}\cdot 0.1CH_2Cl_2\cdot 1.9C_6H_6$ (**4**).

In $6Co^{II}(OEP)\cdot 5C_{60}\cdot 5CH_2Cl_2$ (**1**), $6Zn^{II}(OEP)\cdot 5C_{60}\cdot 5CH_2Cl_2$ (**2**), and $Cu^{II}(OEP)\cdot C_{60}\cdot CH_2Cl_2$ (**3**), the porphyrins display domed distortions with all of the pyrrole nitrogen atoms (and the metal ion) on the side of the porphyrin plane that faces away from the adjacent fullerene. The domed distortion is greatest in all three porphyrins in $6Zn^{II}(OEP)\cdot 5C_{60}\cdot 5CH_2Cl_2$(**2**). Notice that in $6Zn^{II}(OEP)\cdot 5C_{60}\cdot 5CH_2Cl_2$(**2**), the pyrrole rings containing N1, N5, and N11 show the largest out-of-plane distortion. These distortions involve those nitrogen atoms that are utilized in interactions with the zinc ions in the adjacent $Zn^{II}(OEP)$ molecules in the

DOI: 10.1021/acs.cgd.9b01092
Cryst. Growth Des. 2019, 19, 6743−6751

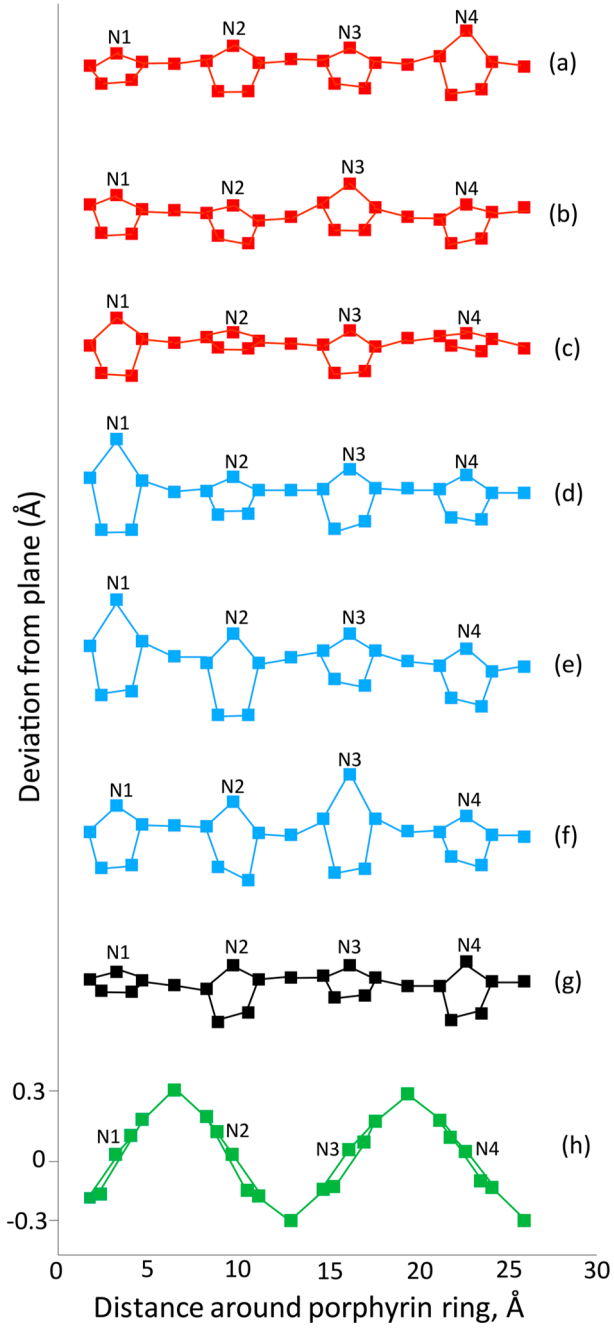

Figure 6. Diagrams comparing the out-of-plane displacements of the porphyrin core atoms from the mean plane of the porphyrin for $6Co^{II}(OEP)\cdot 5C_{60}\cdot 5CH_2Cl_2$ (**1**), (a, b, c) in red; $6Zn^{II}(OEP)\cdot 5C_{60}\cdot 5CH_2Cl_2$ (**2**), (d, e, f) in blue; $Cu^{II}(OEP)\cdot C_{60}\cdot CH_2Cl_2$ (**3**), (g) in black and $Ni^{II}(OEP)\cdot C_{60}\cdot 0.1CH_2Cl_2\cdot 1.9C_6H_6$ (**4**), (h) in green.

dimeric units as shown in Figure 3. In contrast, pristine $Co^{II}(OEP)$, $Zn^{II}(OEP)$, $Cu^{II}(OEP)$, and the triclinic polymorphs of $Ni^{II}(OEP)$ have very small distortions from planarity as shown in Figure 7.

The structure of $Ni^{II}(OEP)\cdot C_{60}\cdot 0.1CH_2Cl_2\cdot 1.9C_6H_6$ (**4**) is unique in that the porphyrin does not show a domed distortion. Rather, in $Ni^{II}(OEP)\cdot C_{60}\cdot 0.1CH_2Cl_2\cdot 1.9C_6H_6$ (**4**) the porphyrin has a saddled distortion that has the largest deviation from planarity of any of the porphyrins in the cocrystals reported here as seen in Figure 6. Despite that distortion, the nickel ion resides closer to the N_4 plane than

Table 3. Metal−Nitrogen Distances (Å) in Cocrystals

$6Co^{II}(OEP)\cdot 5C_{60}\cdot 5CH_2Cl_2$ (**1**)		$6Zn^{II}(OEP)\cdot 5C_{60}\cdot 5CH_2Cl_2$ (**2**)	
Co1−N1	1.972(6)	Zn1−N1	2.076(4)
Co1−N2	1.965(6)	Zn1−N2	2.053(5)
Co1−N3	1.978(6	Zn1−N3	2.028(4)
Co1−N4	1.970(6)	Zn1−N4	2.049(5)
Co1−N_4 plane	0.039(3)	Zn1−N_4 plane	0.204(2)
Co2−N5	1.965(6)	Zn2−N5	2.086(4)
Co2−N6	1.982(6)	Zn2−N6	2.051(5)
Co2−N7	1.966(6)	Zn2−N7	2.039(4)
Co2−N8	1.971(6)	Zn2−N8	2.047(5)
Co2−N_4 plane	0.016(3)	Zn2−N_4 plane	0.207(2)
Co3−N9	1.979(6)	Zn3−N9	2.034(4)
Co3−N10	1.970(6)	Zn3−N10	2.047(5)
Co3−N11	1.965(6)	Zn3−N11	2.095(4)
Co3−N12	1.967(6)	Zn3−N12	2.042(5)
Co3−N_4 plane	0.034(3)	Zn3−N_4 plane	0.215(2)
$Cu^{II}(OEP)\cdot C_{60}\cdot CH_2Cl_2$ (**3**)		$Ni^{II}(OEP)\cdot C_{60}\cdot 0.1CH_2Cl_2\cdot 1.9C_6H_6$ (**4**)	
Cu1−N1	2.006(2)	Ni1−N1	1.9482(10)
Cu1−N2	1.999(2)	Ni1−N2	1.9525(10)
Cu1−N3	2.011(2)	Ni1−N3	1.9496(10)
Cu1−N4	2.006(2)	Ni1−N4	1.9549(10)
Cu1−N_4 plane	0.0791(11)	Ni1−N_4 plane	0.0128(5)

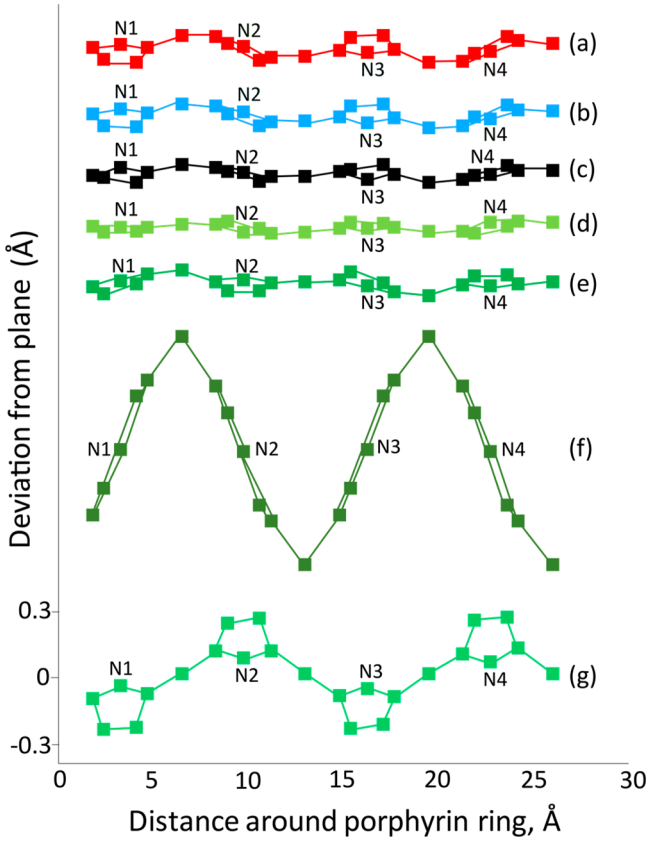

Figure 7. Diagrams comparing the out-of-plane displacements of the porphyrin core atoms from the mean plane of the porphyrin for $Co^{II}(OEP)$ (a) in red (ref 44); $Zn^{II}(OEP)$ (b) in blue (ref 45); $Cu^{II}(OEP)$ (c) in black (ref 46) and polymorphs of $Ni^{II}(OEP)$: (d) (ref 47), (e) (ref 48), (f) (ref 49), and (g) (ref 50) in shades of green.

any other of the metal ions considered here, with a deviation from the plane of only 0.0128(5) Å. The most extreme case is

DOI: 10.1021/acs.cgd.9b01092
Cryst. Growth Des. 2019, 19, 6743−6751

that of Zn, which deviates from the N4 plane by an average (of three Zn atoms) of 0.209(2) Å.

CONCLUSIONS

Mixing of solutions of $M^{II}(OEP)$ with M = Co, Ni, Cu dissolved in dichloromethane and C_{60} in benzene produced four different types of cocrystals with each metal ion producing a different structure. In all cases, the $M^{II}(OEP)$ molecules crystallize as back-to-back pairs, but varying numbers of ethyl groups embracing the adjacent C_{60} molecule. Nevertheless, in the structures reported here, all of the fullerene molecules are ordered at 90 K. In the crystals of $6Co^{II}(OEP)\cdot 5C_{60}\cdot 5CH_2Cl_2$ (**1**) and $6Zn^{II}(OEP)\cdot 5C_{60}\cdot 5CH_2Cl_2$ (**2**), the thermal parameters for the fullerenes show that thermal motion is the least when the fullerene is surrounded by two porphyrins and the greatest when there is no porphyrin near the C_{60} cage. Cocrystallization produces changes in the planarity of the $M^{II}(OEP)$ molecules with the zinc, cobalt, and copper porphyrins undergoing a dome distortion that puts the metal further from the fullerene. The $Ni^{II}(OEP)$ molecule in $Ni^{II}(OEP)\cdot C_{60}\cdot 0.1CH_2Cl_2\cdot 1.9C_6H_6$ (**4**) shows a ruffled distortion that is the largest out-of-plane distortion seen in these cocrystals but is smaller than that found in the tetragonal polymorph of pristine $Ni^{II}(OEP)$.[39]

EXPERIMENTAL SECTION

Materials and General Consideration. $Ni^{II}(OEP)$ and $H_2(OEP)$ were purchased from Frontier Scientific. Metalation of $H_2(OEP)$ was accomplished by an established route.[51] C_{60} and C_{70} were purchased from SES Research with 99.5% and 99% purity, respectively. Solvents were obtained commercially and used as received.

Crystal Growth. In a clean scintillation vial, a 0.56 mmol solution of C_{60} in benzene was prepared by sonication for approximately 30 min. In a separate scintillation vial, an equal volume of a 0.56 mmol solution of $M^{II}(OEP)$ in dichloromethane was prepared. Cocrystallization was conducted in sterile, thick-walled glass tubes with an approximate inner volume of 2.0 mL. A 1.0 mL portion of the $M^{II}(OEP)$ solution in dichloromethane was slowly pipetted into the tube through a filter pipet. Next, 1.0 mL of the C_{60} solution in benzene is carefully layered over the $M^{II}(OEP)$ solution through a fresh filter pipet. For each combination of metalloporphyrins, additional tubes were prepared by addition of the C_{60} solution in benzene to the tube with subsequent addition of the $M^{II}(OEP)$ solution in dichloromethane. In this case, the $M^{II}(OEP)$ solution in dichloromethane sank through the benzene solution with concomitant mixing of the solutions. The crystal tubes were capped with a rubber septum and left undisturbed in dark cabinet until suitable crystal growth occurred. The yields of crystals were $6Co^{II}(OEP)\cdot 5C_{60}\cdot 5CH_2Cl_2$ (**2**), 20%; $6Zn^{II}(OEP)\cdot 5C_{60}\cdot 5CH_2Cl_2$ (**2**), 20%; $Cu^{II}(OEP)\cdot C_{60}\cdot CH_2Cl_2$ (**3**), 80%; $Ni^{II}(OEP)\cdot C_{60}\cdot 0.1CH_2Cl_2\cdot 1.9C_6H_6$ (**4**), 50%. These yields were not optimized. The variation results from the harvesting of crystals at different times during crystal growth. Regardless of growth time, inspection of all samples indicated that only the phase reported here was present.

Crystal Structure Determinations. A black needle of $6Zn^{II}(OEP)\cdot 5C_{60}\cdot 5CH_2Cl_2$ (**2**) was mounted in the 90 K nitrogen cold stream provided by an Oxford Cryostream low-temperature apparatus on the goniometer head of a Bruker D8 diffractometer equipped with an PHOTON II CMOS detector on beamline 12.2.1 at the Advanced Light Source (Lawrence Berkeley National Laboratory, Berkeley, CA). Data were collected with the use of synchrotron radiation (λ = 0.7288 Å). A crystal of $6Co^{II}(OEP)\cdot 5C_{60}\cdot 5CH_2Cl_2$ (**1**) (black lath) was mounted in the 90 K nitrogen cold stream provided by a CRYO Industries low-temperature apparatus on a Bruker Kappa DUO instrument equipped with a molybdenum microsource (λ = 0.71073 Å). Black blocks of $Cu^{II}(OEP)\cdot C_{60}\cdot CH_2Cl_2$ (**3**) and $Ni^{II}(OEP)\cdot C_{60}\cdot 0.1CH_2Cl_2\cdot 1.9C_6H_6$ (**4**) were mounted similarly on a Bruker Apex II employing a fine-focus Mo sealed tube, (λ = 0.71073 Å). All data sets were reduced with the use of Bruker SAINT,[52] and a multiscan absorption correction was applied with the use of SADABS. Structure solutions and refinements were conducted with SHELXT-2015[53] and SHELXL-2018,[54] respectively. Crystallographic data are reported in Tables 1 and 2.

ASSOCIATED CONTENT

Supporting Information

The Supporting Information is available free of charge on the ACS Publications website at DOI: 10.1021/acs.cgd.9b01092.

Additional figures and numbering schemes for the porphyrin crystal structures (PDF)

Accession Codes

CCDC 1947013−1947018 contain the supplementary crystallographic data for this paper. These data can be obtained free of charge via www.ccdc.cam.ac.uk/data_request/cif, or by emailing data_request@ccdc.cam.ac.uk, or by contacting The Cambridge Crystallographic Data Centre, 12 Union Road, Cambridge CB2 1EZ, UK; fax: +44 1223 336033.

AUTHOR INFORMATION

Corresponding Authors

*(M.M.O.) E-mail: mmolmstead@ucdavis.edu. Telephone: (530) 752-6668. Fax: (530) 752-8995.

*(A.L.B.) E-mail: albalch@ucdavis.edu. Telephone: (530) 752-0941. Fax: (530) 752-8995.

ORCID

Marilyn M. Olmstead: 0000-0002-6160-1622

Alan L. Balch: 0000-0002-8813-6281

Notes

The authors declare no competing financial interest.

ACKNOWLEDGMENTS

We thank the Advanced Light Source, supported by the Director, Office of Science, Office of Basic Energy Sciences, of the U.S. Department of Energy under Contract DE-AC02-05CH11231, for beam time, and the National Science Foundation for financial support (Grant CHE 1807637 to A.L.B. and M.M.O.).

REFERENCES

(1) Kroto, H. W.; Heath, J. R.; O'Brien, S. C.; Curl, R. F.; Smalley, R. E. C_{60} - Buckminsterfullerene. *Nature* **1985**, *318*, 162−163.

(2) Heath, J. R.; O'Brien, S. C.; Zhang, Q.; Liu, Y.; Curl, R. F.; Kroto, H. W.; Tittel, F. K.; Smalley, R. E. Lanthanum Complexes of Spheroidal Carbon Shells. *J. Am. Chem. Soc.* **1985**, *107*, 7779−7780.

(3) Krätschmer, W.; Lamb, L. D.; Fostiropoulos, K.; Huffman, D. R. Solid C_{60}: a new form of carbon. *Nature* **1990**, *347*, 354−358.

(4) Cox, D. M.; Trevor, D. J.; Reichmann, K. C.; Kaldor, A. $C_{60}La$: A Deflated Soccer Ball? *Chem. Informationsdienst* **1986**, *17*, 2458−2459.

(5) Hawkins, J. M.; Meyer, A.; Lewis, T. A.; Loren, S.; Hollander, F. J. Crystal structure of osmylated C_{60}: confirmation of the soccer ball framework. *Science* **1991**, *252*, 312−314.

(6) Fagan, P. J.; Calabrese, J. C.; Malone, B. The Chemical Nature of Buckminsterfullerene (C_{60}) and the Characterization of a Platinum Derivative. *Science* **1991**, *252*, 1160−1161.

(7) Balch, A. L.; Catalano, V. J.; Lee, J. W.; Olmstead, M. M.; Parkin, S. R. (η^2-C_{70})Ir(CO)Cl(PPh_3)$_2$. The Synthesis and Structure of an Organometallic Derivative of a Higher Fullerene. *J. Am. Chem. Soc.* **1991**, *113*, 8953−8954.

(8) Balch, A. L.; Ginwalla, A. S.; Lee, J. W.; Noll, B. C.; Olmstead, M. M. Partial Separation and Structural Characterization of C_{84}

DOI: 10.1021/acs.cgd.9b01092
Cryst. Growth Des. 2019, 19, 6743−6751

Isomers by Crystallization of $(\eta^2$-$C_{84})Ir(CO)Cl(P(C_6H_5)_3)_2$. *J. Am. Chem. Soc.* **1994**, *116*, 2227−2228.
(9) Filatov, A. S.; Ferguson, M. V.; Spisak, S. N.; Li, B.; Campana, C. F.; Petrukhina, M. A. Bowl-Shaped Polyarenes as Concave−Convex Shape Complementary Hosts for C_{60}- and C_{70}- Fullerenes. *Cryst. Growth Des.* **2014**, *14*, 756−762.
(10) Ghiassi, K. B.; Chen, S. Y.; Prinz, P.; de Meijere, A.; Olmstead, M. M.; Balch, A. L. Cocrystallization of C_{60} or C_{70} with the Bowl-Shaped Hydrocarbon Hexakis[(*E*)-3,3-dimethyl-1-butenyl]benzene To Form Chains of Clamshell Assemblies. *Cryst. Growth Des.* **2014**, *14*, 4005−4010.
(11) King, B. T.; Olmstead, M. M.; Baldridge, K. K.; Kumar, B.; Balch, A. L.; Gharamaleki, J. A. Molecular nesting in co-crystals of tetrabenzoquadrannulene and C_{60}: application of the sphere in a cone model. *Chem. Commun.* **2012**, *48*, 9882−9884.
(12) Olmstead, M. M.; Costa, D. A.; Maitra, K.; Noll, B. C.; Phillips, S. L.; Van Calcar, P. M.; Balch, A. L. Interaction of Curved and Flat Molecular Surfaces. The Structures of Crystalline Compounds Composed of Fullerene (C_{60}, $C_{60}O$, C_{70}, and $C_{120}O$) and Metal Octaethylporphyrin Units. *J. Am. Chem. Soc.* **1999**, *121*, 7090−7097.
(13) Stevenson, S.; Rice, G.; Glass, T.; Harich, K.; Cromer, F.; Jordan, M. R.; Craft, J.; Hadju, E.; Bible, R.; Olmstead, M. M.; Maitra, K.; Fisher, A. J.; Balch, A. L.; Dorn, H. C. Small-bandgap endohedral metallofullerenes in high yield and purity. *Nature* **1999**, *401*, 55−57.
(14) Zhang, Y. K. B.; Ghiassi, K. B.; Deng, Q.; Samoylova, N. A.; Olmstead, M. M.; Balch, A. L.; Popov, A. A. Synthesis and Structure of $LaSc_2N@C_s(hept)$-C_{80} with One Heptagon and Thirteen Pentagons. *Angew. Chem., Int. Ed.* **2015**, *54*, 495−499.
(15) Chen, C.-H.; Abella, L.; Cerón, M. R.; Guerrero-Ayala, M. A.; Rodríguez-Fortea, A.; Olmstead, M. M.; Powers, X. B.; Balch, A. L.; Poblet, J. M.; Echegoyen, L. Zigzag Sc_2C_2 Carbide Cluster inside a [88]Fullerene Cage with One Heptagon, $Sc_2C_2@C_s(hept)$-C_{88}: A Kinetically Trapped Fullerene Formed by C2 Insertion? *J. Am. Chem. Soc.* **2016**, *138*, 13030−13037.
(16) Yamada, M.; Kurihara, H.; Suzuki, M.; Guo, J. D.; Waelchli, M.; Olmstead, M. M.; Balch, A. L.; Nagase, S.; Maeda, Y.; Hasegawa, T.; Lu, X.; Akasaka, T. $Sc_2@C_{66}$ Revisited: An Endohedral Fullerene with Scandium Ions Nestled within Two Unsaturated Linear Triquinanes. *J. Am. Chem. Soc.* **2014**, *136*, 7611−7614.
(17) Stevenson, S.; Mackey, M. A.; Stuart, M. A.; Phillips, J. P.; Easterling, M. L.; Chancellor, C. J.; Olmstead, M. M.; Balch, A. L. A Distorted Tetrahedral Metal Oxide Cluster inside an Icosahedral Carbon Cage, Synthesis, Isolation, and Structural Characterization of $Sc_4(\mu_3$-$O)_2@I_h$-C_{80}. *J. Am. Chem. Soc.* **2008**, *130*, 11844−11845.
(18) Valencia, R.; Rodriguez-Fortea, A.; Stevenson, S.; Balch, A. L.; Poblet, J. M. Electronic Structures of Scandium Oxide Endohedral Metallofullerenes, $Sc_4(\mu_3$-$O)_n@I_hC_{80}$(n = 2, 3). *Inorg. Chem.* **2009**, *48*, 5957−5961.
(19) Mercado, B. Q.; Stuart, M. A.; Mackey, M. A.; Pickens, J. E.; Confait, B. S.; Stevenson, S.; Easterling, M. L.; Valencia, R.; Rodriguez-Fortea, A.; Poblet, J. M.; Olmstead, M. M.; Balch, A. L. $Sc_2(\mu_2$-$O)@C_s(6)$-C_{82} and the Relevance of the Thermal and Entropic Effects in Fullerene Isomer Selection. *J. Am. Chem. Soc.* **2010**, *132*, 12098−12105.
(20) Pan, C.; Shen, W.; Yang, L.; Bao, L.; Wei, Z.; Jin, P.; Fang, H.; Xie, Y.; Akasaka, T.; Lu, X. Crystallographic characterization of Y_2C_{2n} (2n = 82, 88−94): direct Y−Y bonding and cage-dependent cluster evolution. *Chem. Sci.* **2019**, *10*, 4707−4713.
(21) Bloodworth, S.; Sitinova, G.; Alom, S.; Vidal, S.; Bacanu, G. R.; Elliott, S. J.; Light, M. E.; Herniman, J. M.; Langley, G. J.; Levitt, M. H.; Whitby, R. J. First Synthesis and Characterization of $CH_4@C_{60}$. *Angew. Chem., Int. Ed.* **2019**, *58*, 5038−5043.
(22) Krylov, D. S.; Liu, F.; Brandenburg, A.; Spree, L.; Bon, V.; Kaskel, S.; Wolter, A. U. B.; Buchner, B.; Avdoshenko, S. M.; Popov, A. A. Magnetization relaxation in the single-ion magnet $DySc_2N@C_{80}$: quantum tunneling, magnetic dilution, and unconventional temperature dependence. *Phys. Chem. Chem. Phys.* **2018**, *20*, 11656−11672.
(23) Zhang, R.; Murata, M.; Aharen, T.; Wakamiya, A.; Shimoaka, T.; Hasegawa, T.; Murata, Y. Synthesis of a distinct water dimer inside fullerene C_{70}. *Nat. Chem.* **2016**, *8*, 435−441.
(24) Konarev, D. V.; Khasanov, S. S.; Otsuka, A.; Saito, G.; Lyubovskaya, R. N. Peculiarities of $C_{60}^{\cdot-}$ Coordination to Cobalt(II) Octaethylporphyrin in Ionic Multicomponent Complexes: Observation of the Reversible Formation of Co-C(C_{60}^-) Coordination Bonds. *Chem. - Eur. J.* **2006**, *12*, 5225−5230.
(25) Bao, L.; Yu, P.; Pan, C.; Shen, W.; Lu, X. Crystallographic identification of $Eu@C_{2n}$ (2n = 88, 86 and 84): completing a transformation map for existing metallofullerenes. *Chem. Sci.* **2019**, *10*, 2153−2158.
(26) Liu, F.; Jin, F.; Wang, S.; Popov, A. A.; Yang, S. F. Pyramidal $TiTb_2C$ cluster encapsulated within the popular $I_h(7)$-C_{80} fullerene cage. *Inorg. Chim. Acta* **2017**, *468*, 203−208.
(27) Liu, F.; Wang, S.; Guan, J.; Wei, T.; Zeng, M.; Yang, S.-F. Putting a Terbium-Monometallic Cyanide Cluster into the C_{82} Fullerene Cage: $TbCN@C_2(5)$-C_{82}. *Inorg. Chem.* **2014**, *53*, 5201−5205.
(28) Zhang, X.; Li, W.; Feng, L.; Chen, X.; Hansen, A.; Grimme, S.; Fortier, S.; Sergentu, D.-C.; Duignan, T. J.; Autschbach, J.; Wang, S.; Wang, Y.; Velkos, G.; Popov, A. A.; Aghdassi, N.; Duhm, S.; Li, X.; Li, J.; Echegoyen, L.; Schwarz, W. H. E.; Chen, N. A diuranium carbide cluster stabilized inside a C_{80} fullerene cage. *Nat. Commun.* **2018**, *9*, 2753.
(29) Karunanithi, K.; Bhyrappa, P. Structural elucidation of a few electron-deficient porphyrin/fullerene cocrystallates: Effect of fullerene on the porphyrin ring conformation. *Inorg. Chim. Acta* **2015**, *427*, 41−51.
(30) Olmstead, M. M.; Nurco, D. J. Fluorinated Tetraphenylporphyrins as Cocrystallizing Agents for C_{60} and C_{70}. *Cryst. Growth Des.* **2006**, *6*, 109−114.
(31) Konarev, D. V.; Neretin, I. S.; Slovokhotov, Y. L.; Yudanova, E. I.; Drichko, N. V.; Shul'ga, Y. M.; Tarasov, B. P.; Gumanov, L. L.; Batsanov, A. S.; Howard, J. A. K.; Lyubovskaya, R. N. New Molecular Complexes of Fullerenes C_{60} and C_{70} with Tetrphenylporphyrins [M(tpp)], in which M = H_2, Mn, Co, Cu, Zn, and FeCl. *Chem. - Eur. J.* **2001**, *7*, 2605−2616.
(32) Balch, A. L.; Lee, J. W.; Noll, B. C.; Olmstead, M. M. A Double Addition Product of C_{60}: $C_{60}\{Ir(CO)Cl(PMe_2Ph)_2\}_2$. Individual Crystallization of Two Conformational Isomers. *J. Am. Chem. Soc.* **1992**, *114*, 10984−10985.
(33) Ghiassi, K. B.; Chen, S. Y.; Wescott, J.; Balch, A. L.; Olmstead, M. M. New Insights into the Structural Complexity of C_{60} $2S_8$: Two Crystal Morphologies, Two Phase Changes, Four Polymorphs. *Cryst. Growth Des.* **2015**, *15*, 404−410.
(34) Wang, Z.; Yang, H.; Jiang, A.; Liu, Z.; Olmstead, M. M.; Balch, A. L. Structural Similarities in $C_s(16)$-C_{86} and $C_2(17)$-C_{86}. *Chem. Commun.* **2010**, *46*, 5262−5264.
(35) Stevenson, S.; Phillips, J. P.; Reid, J. E.; Olmstead, M. M.; Rath, S. P.; Balch, A. L. Pyramidalization of Gd_3N inside a C_{80} cage. The synthesis and structure of $Gd_3N@C_{80}$. *Chem. Commun.* **2004**, 2814−2815.
(36) Yang, J.; Beavers, C. M.; Wang, Z.; Jiang, A.; Liu, Z.; Jin, H.; Mercado, B. Q.; Olmstead, M. M.; Balch, A. L. Isolation of a Small Carbon Nanotube: The Surprising Appearance of $D_{5h}(1)$-C_{90}. *Angew. Chem., Int. Ed.* **2010**, *49*, 886−890.
(37) Dubrovin, V.; Gan, L.-H.; Büchner, B.; Popov, A. A.; Avdoshenko, S. M. Endohedral metal-nitride cluster ordering in metallofullerene−Ni^{II} complexes and crystals: a theoretical study. *Phys. Chem. Chem. Phys.* **2019**, *21*, 8197−8200.
(38) Konarev, D. V.; Khasanov, S. S.; Saito, G.; Lyubovskaya, R. Design of Molecular and Ionic Complexes of Fullerene C_{60} with Metal(II) Octaethylporphyrins, $M^{II}OEP$ (M = Zn, Co, Fe, and Mn) Containing Coordination M-N(ligand) and M-C(C_{60}^-) Bonds. *Cryst. Growth Des.* **2009**, *9*, 1170−1181.
(39) Groom, C. R.; Bruno, I. J.; Lightfoot, M. P.; Ward, S. C. The Cambridge Structural Database (CSD). *Acta Crystallogr., Sect. B: Struct. Sci., Cryst. Eng. Mater.* **2016**, *72*, 171−179.

DOI: 10.1021/acs.cgd.9b01092
Cryst. Growth Des. 2019, 19, 6743−6751

(40) Cullen, D. L.; Meyer, E. F., Jr. The Crystal and Molecular Structure of 2,3,7,8,12,13,17,18-Octaethylporphinatomonopyridinezinc(II). *Acta Crystallogr., Sect. B: Struct. Crystallogr. Cryst. Chem.* **1976**, *32*, 2259−2269.
(41) Lee, H. M.; Olmstead, M. M.; Suetsuna, T.; Shimotani, H.; Dragoe, N.; Cross, R. J.; Kitazawa, K.; Balch, A. L. Crystallographic characterization of Kr@C_{60} in (0.09Kr@C_{60}/0.91C_{60})·{Ni^{II}(OEP)}·2C_6H_6. *Chem. Commun.* **2002**, 1352−1353.
(42) Ishii, T.; Aizawa, N.; Yamashita, M.; Matsuzaka, H.; Kodama, T.; Kikuchi, K.; Ikemoto, I.; Iwasa, Y. First syntheses of cocrystallites consisting of anti-formed metal octaethylporphyrins with fullerene C_{60}. *J. Chem. Soc., Dalton Trans.* **2000**, 4407−4412.
(43) Shelnutt, J. A.; Song, X.-Z.; Ma, J.-G.; Jia, S.-G.; Jentzen, W.; Medforth, C. Nonplanar porphyrins and their significance in proteins. *Chem. Soc. Rev.* **1998**, *27*, 31−41.
(44) Scheidt, W. R.; Turowska-Tyrk, I. Crystal and Molecular Structure of (Octaethylporphinato)cobalt(II). Comparison of the Structures of Four-Coordinate M(TPP) and M(OEP) Derivatives (M = Fe-Cu). Use of Area Detector Data. *Inorg. Chem.* **1994**, *33*, 1314−1318.
(45) Ozarowski, A.; Lee, H. M.; Balch, A. L. Crystal Environments Probed by EPR Spectroscopy. Variations in the EPR Spectra of Co^{II}(octaethylporphyrin) Doped in Crystalline Diamagnetic Hosts and a Reassessment of the Electronic Structure of Four-Coordinate Cobalt(II). *J. Am. Chem. Soc.* **2003**, *125*, 12606−12614.
(46) Pak, R.; Scheidt, W. R. Structure of (2,3,7,8,12,13,17,18-Octaethylporphinato)copper(II). *Acta Crystallogr., Sect. C: Cryst. Struct. Commun.* **1991**, *47*, 431−433.
(47) Cullen, D. L.; Meyer, E. F., Jr. Crystal and Molecular Structure of the Triclinic Form of l,2,3,4,5,6,7,8-Octaethylporphinatonickel(II). A Comparison with the Tetragonal Form. *J. Am. Chem. Soc.* **1974**, *96*, 2095−2102.
(48) Brennan, T. D.; Scheidt, W. R.; Shelnutt, J. A. New Crystalline Phase of (Octaethylporphinato)nickel(II). Effects of π-π Interactions on Molecular Structure and Resonance Raman Spectra. *J. Am. Chem. Soc.* **1988**, *110*, 3919−3924.
(49) Meyer, E. F., Jr. The Crystal and Molecular Structure of Nickel(II)octaethylporphyrin. *Acta Crystallogr., Sect. B: Struct. Crystallogr. Cryst. Chem.* **1972**, *28*, 2162−2167.
(50) Bernal, I. *CSD Communication*; CAMJIM, CCDC 644767.
(51) Asano, M.; Kaizu, Y.; Kobayashi, H. The lowest excited states of copper porphyrins. *J. Chem. Phys.* **1988**, *89*, 6567−6576.
(52) *SAINT and SADABS*; Bruker AXS Inc.: Madison, WI, 2018.
(53) SHELXT: Sheldrick, G. M. *Acta Crystallogr., Sect. A: Found. Adv.* **2015**, *71*, 3−8.
(54) SHELXL: Sheldrick, G. M. *Acta Crystallogr., Sect. C: Struct. Chem.* **2015**, *71*, 3−8.

DOI: 10.1021/acs.cgd.9b01092
Cryst. Growth Des. 2019, 19, 6743−6751